

Influence of chirality on the electron transmission through step-like potential in zigzag, armchair, and $(2m,m)$ carbon nanotubes

Lyuba Malysheva*

Bogolyubov Institute for Theoretical Physics, 03680 Kiev, Ukraine

(Dated: November 4, 2021)

We report the one-electron spectrum and eigenstates of infinite achiral and chiral $(2m,m)$ carbon nanotubes found by using the analytic solution to the Schrödinger equation for the tight-binding Hückel-type Hamiltonian. With the help of matching the wave functions on the interfaces between the regions, where electrons have different site energies, we find and compare the transmission coefficients for zigzag, armchair and chiral nanotubes subjected to the action of an applied step-like potential. The correspondence between the nanotube band structure and the energy dependence of the transmission coefficient is demonstrated. It is shown that the $(2m,m)$ nanotubes with a medium chiral angle reveal intermediate transport properties as compared with the achiral armchair, and zigzag nanotubes.

I. INTRODUCTION

The unique spectroscopic and electron-transport properties of carbon nanotubes (CNTs) explain the continuous efforts of experimentalists and theoreticians aimed at the production and investigation of CNT- and graphene-based electronic devices. Discovered in the early nineties [1], the carbon nanotubes are now widely used in biomedical applications [2] and in energy storage facilities [3], thin-film electronics [4], as well as in the production of carbon nanotube computers, transistors, and sensors [5–7].

The comprehensive theoretic investigations of the electron and transport properties of CNTs [8, 9] started shortly after their experimental discovery. In recent years, the continued theoretical investigations of CNTs have been mainly performed within the Dirac relativistic [10–12] and Schrödinger nonrelativistic [13–20] one-particle theories. In this report, we use the nonrelativistic approach: the analytic solution to the Schrödinger equation for the tight-binding Hückel-type Hamiltonian. Our interest is mainly focused on the electronic structure and transport properties both of the well-studied achiral armchair and zigzag CNTs, as well as of the much less investigated chiral nanotubes. To be precise, we consider medium-chiral-angle $(2m,m)$ CNTs with chirality angle equal to 19.1° . This choice is explained both by the relative simplicity of this structure and by the existence of the well-known and experimentally realized procedure of getting nanotubes with chiral indices $(2m,m)$ [21, 22].

Our goal is to find the transmission coefficients for the achiral and chiral CNTs in a potential that has a step-like profile. We start with the solution of the stationary Schrödinger equation $\mathbf{H}\Psi = E\Psi$ with the nearest-neighbor tight-binding Hamiltonian for infinite achiral and chiral nanotubes presented in Fig. 1. We use the one-electron approximation, and the model represents an ideal π electron system. In the nearest-neighbor approximation, for the lattice site enumeration explained in Fig. 1, the electronic properties of CNTs can be well described by the Hückel-type Hamiltonian

$$\mathbf{H} = \sum_{\mathbf{r}'-\mathbf{r}=\mathbf{q}} \sum_{\mathbf{r}} [\varepsilon_{\mathbf{r}}(1 - \delta_{\mathbf{q},0}) - \beta] c_{\mathbf{r}}^{\dagger} c_{\mathbf{r}+\mathbf{q}}, \quad (1)$$

where $c_{\mathbf{r}}^{\dagger}$ ($c_{\mathbf{r}}$) is the electron creation (annihilation) operator at $\mathbf{r} = n_a, n_z, \alpha$; $\varepsilon_{\mathbf{r}}$ and $-\beta$ ($\beta > 0$) are, respectively, the electron site energy and the C–C hopping integral. The wave function of π electron reads $\Psi = \sum_{\mathbf{r}} \psi_{\mathbf{r}} c_{\mathbf{r}}^{\dagger} |0\rangle$, where the expansion coefficients obey the corresponding sets of equations depending on the type of CNTs. The Fermi energy of π electrons is equal to zero and serves as the reference. In what follows, energy is always expressed in the units of β . To solve the problem of particle transmission under a potential with step-like profile, we consider the electron transmission through CNTs with site energies taking the values 0 from the left and U from the right of the interface, as shown in Figs. 1 a–c.

It follows from Fig. 1 that a unit cell of a CNT contains the atoms with labels $\alpha = l, r, \lambda, \rho$ for the zigzag and armchair CNTs, and the atoms with $\alpha = l, r, \lambda, \rho, \omega, \epsilon$ for $(2m,m)$ CNTs. The zigzag nanotube (zCT) can be regarded as a periodic sequence of polyparaphenylene molecules, the armchair nanotube (aCT) consist of the acene chains, and the $(2m,m)$ CNT is formed by the acene chains connected with a simple carbon chain (the building blocks of

* malysheva@bitp.kiev.ua

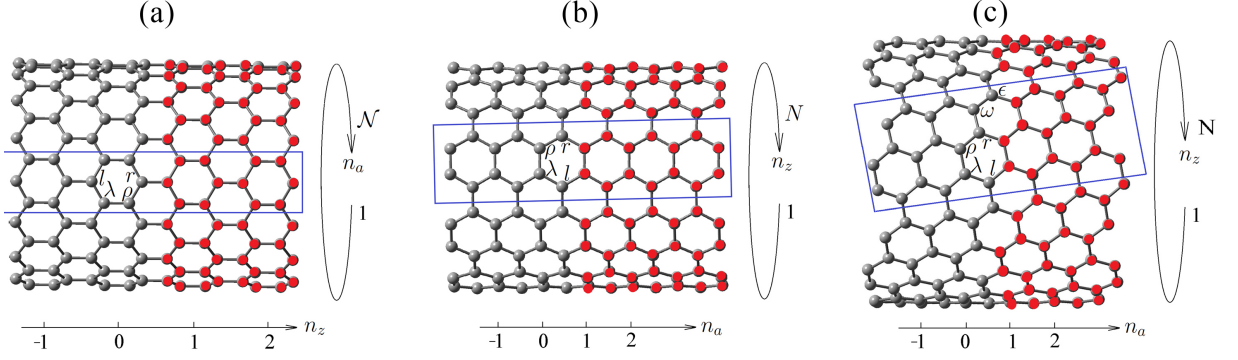


FIG. 1. Fragments of infinite zigzag (a), armchair (b) and $(2m, m)$ CNTs subjected to the step-like potential. The grey and red circles indicate zero and U -shifted site energies of carbon atoms. The labels $\alpha = \lambda, \rho, l, r$ for (a), (b) and $\alpha = \lambda, \rho, l, r, \omega, \epsilon$ for (c) are shown for the atoms with $n_z = 0$ for (a) and with $n_a = 0$ for (b) and (c). The atoms in the frame have one and the same value of the coordinate n_a in (a) and n_z in (b) and (c).

all three CNTs are depicted as blue frames in Fig. 1). As shown earlier [14, 15, 23], the states of π electrons in the considered CNTs can be arranged in \mathcal{N} (zCT), N (aCT), and N ($(2m, m)$ CNT) conduction bands and equal number of valence bands, each of which is subdivided into two (zCT and aCT) and three ($(2m, m)$ CNT) subbands. Due to the orthogonality of transverse wave functions (see Eqs. (4) and (13)), there is no interband transition, and, hence, the problem of finding the transmission coefficient is reduced to the problem of obtaining the scattering amplitudes for each j th (zCT) or ν th (aCT and $(2m, m)$ CNT), see Fig. 1, conduction band. Labeling the wave function to the left and right of the interface by L and R , respectively, we can write the solution to the Schrödinger equation for any incident mode μ as follows (the precise form of these relations is specified for zCTs, aCTs, and $(2m, m)$ CNTs in Sections II and III):

$$\begin{aligned}\psi_{n_a, n_z, \alpha}^L &= \psi_{n_a, n_z, \alpha}(\vec{k}_\mu) + \sum_{\mu_r} R_{\mu_r} \psi_{n_a, n_z, \alpha}(\vec{k}_{\mu_r}), \\ \psi_{n_a, n_z, \alpha}^R &= \sum_{\mu_t} T_{\mu_t} \psi_{n_a, n_z, \alpha}(\vec{k}_{\mu_t}).\end{aligned}\quad (2)$$

In Eqs. (2), the wave vectors are given in a^{-1} units (lattice constant in CNTs $a \approx 2.5\text{\AA}$), summation is carried out over reflected (μ_r) and transmitted (μ_t) modes, and $\psi_{n_a, n_z, \alpha}$ (for any mode) is an eigenstate. The eigenvalues $E(k)$ are found from the dispersion relation. The wave vector marked by the overbar (\vec{k}), as well as the corresponding eigenenergy \bar{E} , refer to the nanotubes with site energies shifted by U : $\bar{E} = E - U$. In what follows, we consider only positive energies $E \geq 0$, while the sign of \bar{E} depends on U .

II. ACHIRAL (ZIGZAG AND ARMCHAIR) CNTS

The system of equations for the wave functions $\psi_{n_a, n_z, \alpha}$ (the meaning of labels is explained in Fig. 1) for both achiral CNTs has the same form

$$\begin{aligned}E\psi_{n_a, n_z, l} &= -\psi_{n_a, n_z, \lambda} - \psi_{n_a+1, n_z, \lambda} - \psi_{n_a, n_z-1, r}, \\ E\psi_{n_a, n_z, \lambda} &= -\psi_{n_a, n_z, l} - \psi_{n_a-1, n_z, l} - \psi_{n_a, n_z, \rho}, \\ E\psi_{n_a, n_z, \rho} &= -\psi_{n_a, n_z, r} - \psi_{n_a-1, n_z, r} - \psi_{n_a, n_z, \lambda}, \\ E\psi_{n_a, n_z, r} &= -\psi_{n_a, n_z, \rho} - \psi_{n_a+1, n_z, \rho} - \psi_{n_a, n_z+1, l},\end{aligned}\quad (3)$$

while the boundary conditions are different for zigzag and armchair nanotubes. We start with the simplest case, a zigzag CNT.

A. Zigzag CNT

A fragment of a zigzag CNT is drawn in Fig. 1a. This nanotube has chiral angle $\theta = 0^\circ$. Using the presented notation, the periodic boundary conditions can be written as $\psi_{0, n_z, l(r)} = \psi_{\mathcal{N}, n_z, l(r)}$, $\psi_{\mathcal{N}+1, n_z, \lambda(\rho)} = \psi_{1, n_z, \lambda(\rho)}$, where

$n_a = 1, \dots, \mathcal{N}$, and $n_z = -\infty, \dots, \infty$, which implies the following form of solutions to the system (3) for $\alpha = \lambda, \rho, l, r$:

$$\psi_{n_a, n_z, \alpha} = \alpha e^{i\xi_j n_a} e^{i\kappa n_z}, \quad \xi_j \equiv \frac{2\pi j}{\mathcal{N}}, \quad j = 1, \dots, \mathcal{N}, \quad (4)$$

and the wave vector κ , $0 \leq k \leq \pi$, is in the units of a^{-1} . The electron structure and quantum transport in the zCTs (and their counterparts, armchair nanoribbons) were considered in a number of works [14, 15, 24–30], and the eigenvalues and eigenstates $\psi_{n_a, n_z, \alpha}$ were found in different representations. The eigenfunctions $\psi_{m, n, \alpha}^{(j)}(k)$ can be found by using different approaches [15, 16, 24]. We use here the following form for the coefficients α in (4):

$$\begin{aligned} l &= \mp \sigma_j \frac{z_j^\pm}{E_j^\pm} e^{-i\kappa_j^\pm/2}, \quad r = 1, \\ \lambda &= \pm \sigma_j e^{-i\pi j/\mathcal{N}} e^{-i\kappa_j^\pm/2}, \quad \rho = -e^{-i\pi j/\mathcal{N}} \frac{z_j^\pm}{E_j^\pm}, \end{aligned} \quad (5)$$

and the corresponding dispersion relation (for zero site energy):

$$(E_j^\pm)^2 = 4 \cos^2 \frac{\pi j}{\mathcal{N}} + 1 \pm 4 \sigma_j \cos \frac{\pi j}{\mathcal{N}} \cos \frac{\kappa}{2} = |z_j^\pm|^2, \quad (6)$$

where

$$z_j^\pm \equiv 2 \cos \frac{\pi j}{\mathcal{N}} \pm \sigma_j e^{-i\frac{\kappa}{2}}, \quad \sigma_j \equiv \sin(\mathcal{N}/2 - j). \quad (7)$$

The sign \pm in Eq. (6) marks the "plus" and "minus" branches of the dependence $E_j(\kappa)$. Note that the mode with the lowest absolute energy belongs to the "minus" branch. It is easy to see that for any j , there are two positive κ (that we denote by κ_j^\pm) satisfying Eq.(6):

$$\begin{aligned} \kappa_j^\pm &= 2 \arccos \left[s \frac{(E_j^\pm)^2 - 4 \cos^2 \frac{\xi_j}{2} - 1}{4 \sigma_j \cos \frac{\xi_j}{2}} \right], \\ s &\equiv \begin{cases} 1, & \text{for } E_j^+ \\ -1, & \text{for } E_j^- \end{cases} \end{aligned} \quad (8)$$

Evidently, if some κ satisfies Eq.(6), the same is true for $-\kappa$. Differentiating E_j^\pm by κ , we find the group velocities of the corresponding eigenstates:

$$\hbar v_\pm = \frac{dE_j^\pm}{d\kappa} = \mp \frac{1}{E} \left| \cos \frac{\xi_j}{2} \right| \sin \frac{\kappa_j^\pm}{2}. \quad (9)$$

Positive velocity corresponds to the wave going from left to right. Then, for the "plus" energy branch, $-\kappa_j^\pm$ is chosen for the incident mode, while κ_j^\pm corresponds to the reflected wave, and for the "minus" branch the situation is opposite. Thus, for any incident mode j , relations (2) simplify to

$$\begin{aligned} \psi_{n_a, n_z, \alpha}^L &= \psi_{n_a, n_z, \alpha}(-s\kappa_j^\pm) + R_j^\pm \psi_{n_a, n_z, \alpha}(s\kappa_j^\pm), \\ \psi_{n_a, n_z, \alpha}^R &= T_j^\pm \psi_{n_a, n_z, \alpha}(-\bar{s}\bar{\kappa}_j^\pm) \end{aligned} \quad (10)$$

(to recall, the wave vector marked by the overbar ($\bar{\kappa}_j^\pm$) refer to the zCTs with site energies shifted by U : $\bar{E}_j^\pm = E_j^\pm - U$.) Substituting these relations in the first (for $n_z = 1$) and last (for $n_z = 0$) equations of system (3), we find after some algebra (for details, see [24, 25])

$$\begin{aligned} \mathcal{T}_j^\pm &= |T_j^\pm|^2 \frac{E_j^\pm \sin \frac{\bar{\kappa}_j^\pm}{2}}{\bar{E}_j^\pm \sin \frac{\kappa_j^\pm}{2}} = \frac{16 \cos^2 \frac{\pi j}{\mathcal{N}} \sin \frac{\kappa_j^\pm}{2} \sin \frac{\bar{\kappa}_j^\pm}{2}}{\left| -U^2 + 16 \cos^2 \frac{\pi j}{\mathcal{N}} Q^\pm \right|}, \\ Q^\pm &= \begin{cases} \sin^2 \frac{\kappa_j^\pm + \bar{\kappa}_j^\pm}{4}, & s = \bar{s}, \\ \cos^2 \frac{\kappa_j^\pm + \bar{\kappa}_j^\pm}{4}, & s = -\bar{s}, \end{cases} \end{aligned} \quad (11)$$

where $\bar{s} = 1$ for \bar{E}_j^+ and $\bar{s} = -1$ for \bar{E}_j^- . The main properties of the transmission coefficient, which is equal to the sum of all transmission amplitudes of the propagating transverse modes

$$\mathcal{T}(E) = \sum_{j=1}^{\mathcal{N}} (\mathcal{T}_j^+ + \mathcal{T}_j^-) \quad (12)$$

are discussed in Sec.III.

B. Armchair CNT

A fragment of infinite armchair CNT (aCT), a structure having chiral angle $\theta = 30^\circ$, is drawn in Fig. 1b. For this case, the periodic boundary conditions in the transverse direction can be written as $\psi_{n_a,0,r} = \psi_{n_a,N,r}$, $\psi_{n_a,N+1,l} = \psi_{n_a,1,l}$, where $n_a = -\infty, \dots, \infty$, and $n_z = 1, \dots, N$, which implies the following form of solutions to the system (3) for $\alpha = \lambda, \rho, l, r$:

$$\psi_{n_a, n_z, \alpha} = \alpha e^{i k n_a} e^{i \xi_\nu n_z}, \quad \xi_\nu \equiv \frac{2\pi\nu}{N}, \quad \nu = 1, \dots, N. \quad (13)$$

The energy eigenvalues are found from the condition of solvability of system (3) in the form

$$(E_\nu^\pm)^2 = 4 \cos^2 \frac{k_\nu^\pm}{2} + 1 \pm 4 \sigma_\nu \cos \frac{k_\nu^\pm}{2} \cos \frac{\xi_\nu}{2} = |z_\nu^\pm|^2, \quad (14)$$

where

$$z_\nu^\pm \equiv 2 \cos \frac{k_\nu^\pm}{2} \pm \sigma_\nu e^{-i \frac{\xi_\nu}{2}}, \quad \sigma_\nu \equiv \sin(N/2 - \nu). \quad (15)$$

The corresponding eigenstates evidently coincide with Eqs. (5) with the interchange of transverse and longitudinal quantum numbers: $\xi_j \leftrightarrow k_\nu^\pm$, $\kappa_j^\pm \leftrightarrow \xi_\nu$. The same symmetry exists for the eigenvalues, which is clearly seen from the comparison of Eqs. (6) and (14). However, there is an essential difference between zCT and aCT: for the later, for any energy E and ν , the values of k_ν should be found from the solution to the quadratic equation (14):

$$2 \cos \frac{k_\nu^{1,2}}{2} = \left| \sqrt{E^2 - \sin^2 \frac{\xi_\nu}{2}} \pm \sigma_\nu \cos \frac{\xi_\nu}{2} \right|. \quad (16)$$

Relation (16) gives the following interval where $k_{1,2}$ are real:

$$\sin \frac{\xi_\nu}{2} \leq E \leq \sqrt{5 + 4 \sigma \cos \frac{\xi_\nu}{2}}. \quad (17)$$

For this energy range, we have or four $(\pm k_{1,2})$, or two $(\pm k_1)$ real values of k . From these k , we choose only those for which the velocity is positive (we suppose that the particles moves from left to right). For two energy branches we get two electron velocities:

$$\hbar v_\pm = \frac{dE_\nu^\pm}{dk} = -\frac{1}{E} \sin \frac{k_\nu^\pm}{2} \left(2 \cos \frac{k_\nu^\pm}{2} \pm \sigma_\nu \cos \frac{\xi_\nu}{2} \right). \quad (18)$$

For the "+" energy branch, the velocity is positive for negative k , and vice versa. For the "-" energy branch, the velocity is negative for k starting from $-\pi$ up to k satisfying

$$2 \cos \frac{k}{2} = \sigma_\nu \cos \frac{\xi_\nu}{2}, \quad (19)$$

for which the velocity becomes positive, up to $k = 0$. Then for $k > 0$, up to k satisfying equality (19), the velocity is negative, and for larger k up to $k = \pi$ it is positive.

Thus, to determine the transmission amplitudes, we first find four solutions to Eq.(16), choose only real solutions (two or four), and choose those k for which the velocity (18) is positive. They are denoted by \vec{k}_1, \vec{k}_2 and/or \vec{k}_1, \vec{k}_2 . If some k_ν and/or \bar{k}_ν are complex, then for the wave going from left to right, we choose those k whose imagine parts are

positive (then, these evanescent waves vanish with increasing n and do not participate in the process of transmission). For reflection, we choose the waves going in the opposite direction: $\vec{k}_1 = -\vec{k}_1, \vec{k}_2 = -\vec{k}_2$, for which the velocities (18) are negative (real k) or whose imaginary parts are negative (complex k).

Since for any energy and ν there are at most two incident modes (numbered by $\nu_0 \leq 2$), solution to Eqs. (3) for each ν_0 can be written in a single-mode form

$$\begin{aligned}\psi_{n_a, n_z, \alpha}^L &= \psi_{n_a, n_z, \alpha}(\vec{k}_\nu) + \sum_{\mu=1}^2 R_\nu^\mu \psi_{n_a, n_z, \alpha}(\vec{k}_\mu), \\ \psi_{n_a, n_z, \alpha}^R &= \sum_{\mu=1}^2 T_\nu^\mu \psi_{n_a, n_z, \alpha}(\vec{k}_\mu).\end{aligned}\tag{20}$$

Substituting relations (20) in the following system obtained from (3):

$$\begin{aligned}E\psi_{0, n_z, l}^L &= -\psi_{0, n_z, \lambda}^L - \psi_{1, n_z, \lambda}^R - \psi_{0, n_z-1, r}^L, \\ \bar{E}\psi_{1, n_z, \lambda}^R &= -\psi_{1, n_z, l}^R - \psi_{0, n_z, l}^L - \psi_{1, n_z, \rho}^R, \\ \bar{E}\psi_{1, n_z, \rho}^R &= -\psi_{1, n_z, r}^R - \psi_{0, n_z, r}^L - \psi_{1, n_z, \lambda}^R, \\ E\psi_{0, n_z, r}^L &= -\psi_{0, n_z, \rho}^L - \psi_{1, n_z, \rho}^R - \psi_{0, n_z+1, l}^L,\end{aligned}\tag{21}$$

we get four linear equations for four unknowns $R_\nu^\mu, T_\nu^\mu, \mu = 1, 2$. They allow us to determine the transmission coefficient

$$\mathcal{T}(E) = \sum_{\nu=1}^N (\mathcal{T}_\nu^1 + \mathcal{T}_\nu^2), \quad \mathcal{T}_\nu^\mu = \frac{v_\nu}{v_\nu^\mu} |T_\nu^\mu|^2.\tag{22}$$

To elucidate the role of chirality in the electron transport through step-like potential, in the next section we perform the derivation of $\mathcal{T}(E)$ for the chiral $(2m, m)$ CNTs.

III. CHIRAL $(2m, m)$ CNT

The system of equations for the wave functions for infinite $(2m, m)$ CNTs, whose fragment is depicted in Fig. 1c, can be written as follows [23]:

$$\begin{aligned}E\psi_{n_a, n_z, l} &= -\psi_{n_a, n_z, \lambda} - \psi_{n_a+1, n_z, \lambda} - \psi_{n_a, n_z-1, \epsilon}, \\ E\psi_{n_a, n_z, \lambda} &= -\psi_{n_a, n_z, l} - \psi_{n_a-1, n_z, l} - \psi_{n_a, n_z, \rho}, \\ E\psi_{n_a, n_z, \rho} &= -\psi_{n_a, n_z, r} - \psi_{n_a-1, n_z, r} - \psi_{n_a, n_z, \lambda}, \\ E\psi_{n_a, n_z, r} &= -\psi_{n_a, n_z, \rho} - \psi_{n_a+1, n_z, \rho} - \psi_{n_a, n_z, \omega}, \\ E\psi_{n_a, n_z, \omega} &= -\psi_{n_a, n_z, \epsilon} - \psi_{n_a-1, n_z, \epsilon} - \psi_{n_a, n_z, r}, \\ E\psi_{n_a, n_z, \epsilon} &= -\psi_{n_a, n_z, \omega} - \psi_{n_a+1, n_z, \omega} - \psi_{n_a, n_z+1, l},\end{aligned}\tag{23}$$

where $n_a = -\infty, \dots, \infty$, with the periodic boundary conditions

$$\psi_{n_a, 0, \omega} = \psi_{n_a, N, \omega}, \quad \psi_{n_a, N+1, l} = \psi_{n_a, 1, l}, \quad n_z = 1, \dots, N.\tag{24}$$

To satisfy these boundary conditions, the solution is sought in the form (13) with $\alpha = \lambda, \rho, l, r, \omega, \epsilon, \nu = 1, \dots, N, \pi \leq k \leq \pi$. Substituting this solution in (23), we obtain the dispersion relation for $(2m, m)$ CNTs [23] in the form of three energy branches:

$$\begin{aligned}(E_\nu^\mu)^2 &= 1 + 4 \cos^2 \frac{k}{2} + 4 \cos \frac{k}{2} \cos \left(-\frac{k}{6} + \frac{\xi_\nu}{3} + y_\mu \right) \\ &= |z_\nu^\mu|^2, \quad \mu = 1, 2, 3, \quad \xi_\nu = \frac{2\pi\nu}{N}, \\ y_1 &= 0, \quad y_2 = -\frac{2\pi}{3}, \quad y_3 = \frac{2\pi}{3}, \\ z_\nu^\mu &\equiv 2 \cos \frac{k}{2} + e^{-i\eta_\nu^\mu}, \quad \eta_\nu^\mu \equiv -\frac{k}{6} + \frac{\xi_\nu}{3} + y_\mu.\end{aligned}\tag{25}$$

It is easy to see that the wave numbers k satisfying Eq.(25) can be found from the following equation of the 6th order:

$$\begin{aligned} e^{6ik} + c_1 e^{5ik} + c_2 e^{4ik} + c_3 e^{3ik} + \bar{c}_2 e^{2ik} + \bar{c}_1 e^{ik} + 1 &= 0, \\ c_1 &= 6 - 3E^2 + e^{-i\xi_\nu}, \\ c_2 &= 3(5 - 5E^2 + E^4) + 3e^{-i\xi_\nu} + e^{i\xi_\nu}, \\ c_3 &= 21 - 27E^2 + 9E^4 - E^6 + 6\cos\xi_\nu, \end{aligned} \quad (26)$$

where the overbar denotes complex conjugate. The corresponding eigenstates can be represented as follows:

$$\begin{aligned} l &= -e^{-i\xi_\nu} e^{i\eta_\nu^\mu} \frac{z_\nu^\mu}{E_\nu^\mu}, \quad \lambda = e^{-i\xi_\nu} e^{i\eta_\nu^\mu} e^{-ik/2}, \\ \rho &= -e^{-i\xi_\nu} e^{2i\eta_\nu^\mu} e^{-ik/2} \frac{z_\nu^\mu}{E_\nu^\mu}, \\ r &= e^{-i\eta_\nu^\mu} e^{-ik/2}, \quad \omega = -e^{-ik/2} \frac{z_\nu^\mu}{E_\nu^\mu}, \quad \epsilon = 1. \end{aligned} \quad (27)$$

The electron velocity for the μ th energy branch is obtained by differentiating Eq.(25):

$$\hbar v_\mu = \frac{dE_\nu^\mu}{dk} = \frac{1}{E_\nu^\mu} \left(\frac{1}{3} \cos \frac{k}{2} \sin \eta_\nu^\mu - \sin k - \sin \frac{k}{2} \cos \eta_\nu^\mu \right). \quad (28)$$

Thus, the procedure of finding the transmission coefficient is similar to that described in Sec. II: we find six roots of Eq.(26), choose only real k , find to which branch they belong, and, to choose the waves going from left to right, choose those k for which the velocity v_μ (28) is positive. The maximal number of such k is 3. They are denoted by $\vec{k}_1, \vec{k}_2, \vec{k}_3$ and/or $\vec{k}_1, \vec{k}_2, \vec{k}_3$. For complex k , we choose those whose imagine parts are positive (then we get the evanescent waves vanishing with increasing n and not participating in transmission). For reflection, we choose the waves going from right to left: $\overleftarrow{k}_1, \overleftarrow{k}_2, \overleftarrow{k}_3$, for which v_μ are negative (real k) or whose imagine parts are negative (complex k).

As a result, for any ν , there are at most three incident modes, that are numbered by $\mu_0 \leq 3$. For each μ_0 , solution to Eqs. (1) in a single-mode form is:

$$\psi_{n_a, n_z, \alpha}^L = \psi_{n_a, n_z, \alpha}(k_{\mu_0}^{\rightarrow}) + \sum_{\mu=1}^3 R_\nu^\mu \psi_{n_a, n_z, \alpha}(k_\mu^{\leftarrow}) \quad (29)$$

$$\psi_{n_a, n_z, \alpha}^R = \sum_{\mu=1}^3 T_\nu^\mu \psi_{n_a, n_z, \alpha}(k_\mu^{\rightarrow}). \quad (30)$$

Substituting these solutions in the system

$$\begin{aligned} E\psi_{0, n_z, l}^L &= -\psi_{0, n_z, \lambda}^L - \psi_{1, n_z, \lambda}^R - \psi_{0, n_z-1, \epsilon}^L, \\ \bar{E}\psi_{1, n_z, \lambda}^R &= -\psi_{1, n_z, l}^R - \psi_{0, n_z, l}^L - \psi_{1, n_z, \rho}^R, \\ \bar{E}\psi_{1, n_z, \rho}^R &= -\psi_{1, n_z, r}^R - \psi_{0, n_z, r}^L - \psi_{1, n_z, \lambda}^R, \\ E\psi_{0, n_z, r}^L &= -\psi_{0, n_z, \rho}^L - \psi_{1, n_z, \rho}^R - \psi_{0, n_z, \omega}^L, \\ \bar{E}\psi_{1, n_z, \omega}^R &= -\psi_{1, n_z, \epsilon}^R - \psi_{0, n_z, \epsilon}^L - \psi_{1, n_z, r}^R, \\ E\psi_{0, n_z, \epsilon}^L &= -\psi_{0, n_z, \omega}^L - \psi_{1, n_z, \omega}^R - \psi_{0, n_z+1, l}^L, \end{aligned} \quad (31)$$

we get six linear equations for six unknowns $R_{\nu_0, \nu}^\mu$, $T_{\nu_0, \nu}^\mu$, $\mu = 1, 2, 3$. They allow us to determine the transmission coefficient

$$\mathcal{T}(E) = \sum_{\nu} (\mathcal{T}_\nu^1 + \mathcal{T}_\nu^2 + \mathcal{T}_\nu^3), \quad \mathcal{T}_\nu^\mu = \frac{v_\nu}{v_\nu^\mu} |T_\nu^\mu|^2. \quad (32)$$

Now we have at hand all the necessary expressions for the analysis of the properties of transmission coefficients for all three types of CNTs.

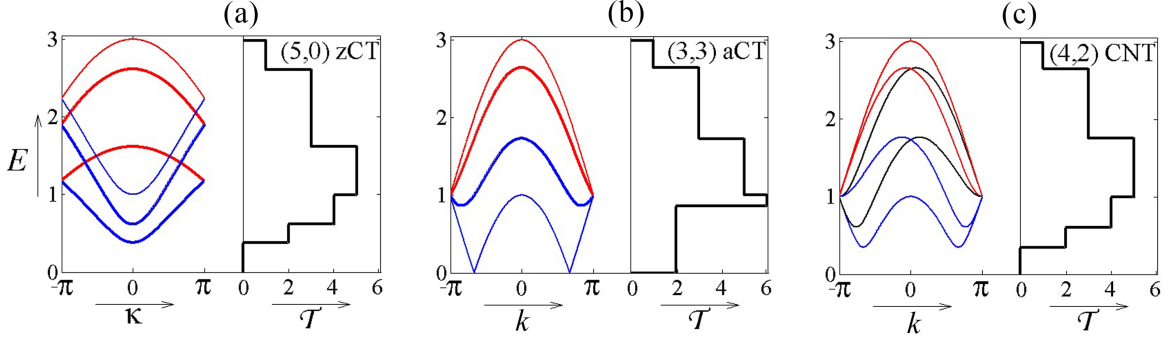


FIG. 2. Electron structure and transmission coefficient for, from left to right, zCT (5,0), aCT (3,3) and chiral (4,2) CNT. Double degenerate modes are drawn by thicker lines. Black curves in the right panel: E_ν^1 ; red curves: E_j^+ (a), E_ν^+ (b), and E_ν^2 (c); blue curves: E_j^- (a), E_ν^- (b), and E_ν^3 (c).

IV. TRANSMISSION COEFFICIENTS

A. Zero potential

It is instructive to start with the discussion of the dependence $\mathcal{T}(E)$ calculated for $U = 0$, when this function is simply equal to the number of "open" modes. In Fig. 2, we plot the dependences $E(k)$ and $E(\kappa)$ and, on the same panel, the corresponding dependences $\mathcal{T}(E)$.

zCTs. For these CNTs, as is well seen in the left panel, that there are no incident modes (and $\mathcal{T} = 0$) if $E < 1 - 2\cos(2\pi/5) = 0.38$, in accordance with Eqs. (6), (7) for $\kappa = 0$. For larger energies, two modes open, since the mode $j = 2$ is doubly degenerate. When $E > |1 - 2\cos(\pi/5)|$, there are four open modes, and, thus, $\mathcal{T} = 4$. The maximal value of \mathcal{T} is equal to 5, and it starts to decrease for $E > 1 + 2\cos(2\pi/5) = 1.62$.

aCTs. Similar trends are observed for the aCT (middle panel), with an essential difference: since the band gap for any aCT is zero, two modes open immediately when E becomes non-zero, and $\mathcal{T} = 2$ up to $E = \sin(\pi/3) = 0.87$, the minimum of the double degenerate "minus" energy branch E_1^- (see Eq.(17)). When E becomes larger than $\sin(\pi/3)$, four modes provided by this energy branch become open and $\mathcal{T} = 6$. For $E > 1$, the number of open modes equals 5 (two from $E_1^- = E_2^-$, two from $E_1^+ = E_2^+$, and one from E_3^+), up to the maximum of E_1^- . With further increase of energy the function $\mathcal{T}(E)$ decreases in a step-like manner, in accordance with the number of open modes.

(2m, m) CTNs. All six modes of (4,2) CNT (right panel) are non-degenerate. As it follows from Eq.(25), the maximal energy value is attained at $k = 0$ for the $\mu = 2$ subbranch with $\nu = N$: $E_{\nu=N}^{\mu=2}(k = 0) = 3$. The energy gap can be estimated as $2E_{\nu=1}^{\mu=3}(k = 2\pi/3) \approx 0.7$. Thus, as is seen in Fig. 2c, $\mathcal{T}(E) = 0$ for $E \lesssim 0.35$. With further increase of E , $\mathcal{T}(E) = 2$ up to the energy equal to the minimum of E_2^3 (or, which is the same, the minimum of E_2^1). The transmission coefficient is maximal, $\mathcal{T}(E) = 5$, for the energies between $E = 1$ and the maximum of E_2^3 (or E_2^1), when all modes are open except E_3^1 . For larger energies, the step-like decrease of \mathcal{T} for all three structure is rather similar.

Thus, as the common features of transmission in all three structure, we can mention the step-like increase with increase of energy up to $E \approx 1$, or, since we use the hopping integral energy units, $E \approx 2.7\text{eV}$. The maximum of \mathcal{T} equals (or is less by 1 then) the whole number of conducting modes. The differences in the behavior of \mathcal{T} for zCTs, aCTs, and chiral CNTs can be expected in the energy region $E \lesssim 1$, while for $E \gtrsim 1$, the three conductance ladders become more and more similar with the energy increase. It can be expected that these regularities remain much the same for small potentials, $U \ll 1$. In the next section, we will see what happens with \mathcal{T} for moderate values of U , taking $U = 0.25$ and $U = 0.5$ as examples.

B. Non-zero potential

Due to the symmetry of the problem, we restrict ourselves to the case $U > 0$ without loss of generality. In Fig. 3 we demonstrate the changes in dependences $\mathcal{T}(E)$ under the step-like potential $U = 0.25$ (i.e., $\sim 0.7\text{ eV}$). Note that the plots of functions $\mathcal{T}(E)$ for zero potential coincide with the corresponding dependences calculated in [31] with the help of the Green function matching technique, providing a useful cross-check on our calculations. Figures 3 and 4 demonstrate that the transmission coefficient $\mathcal{T}(E)$ is always smaller for larger values of U .

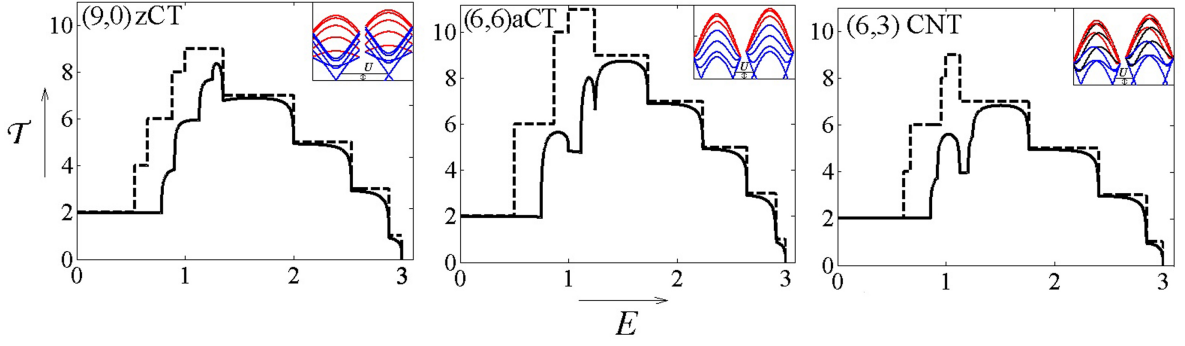


FIG. 3. Transmission coefficient $\mathcal{T}(E)$ for, from left to right, zCT (9,0), aCT (6,6) and chiral (6,3) CNT. Dashed curves: $U = 0$, solid curves: $U = 0.25$. Insets: the corresponding dispersion curves (the colors have the same meaning as in Fig/ 2) for site energies unshifted (left) and shifted by $U = 0.25$ (right).

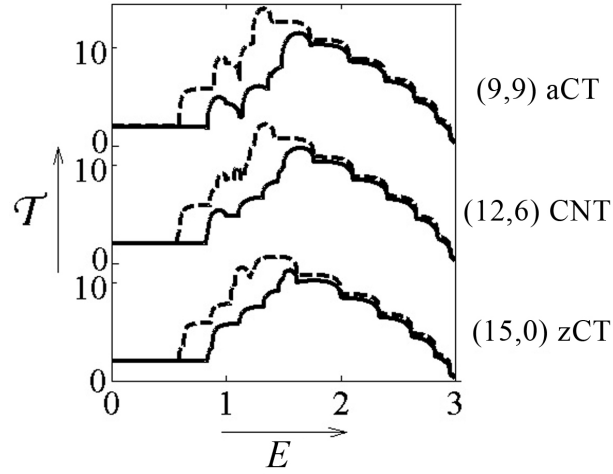


FIG. 4. Transmission coefficient $\mathcal{T}(E)$ for, from bottom to top, zCT (15,0), chiral (12,6) CNT, and aCT (9,9). All three CNTs have close diameters $d \sim 12\text{\AA}$. Dashed curves: $U = 0.25$, solid curves: $U = 0.5$.

As is seen in Fig. 3, for all three types of nanotubes considered here, dependences $\mathcal{T}(E)$ are the same for $E \lesssim 0.5$, namely, $\mathcal{T}(E) = 2$ with a good accuracy for both values $U = 0$ and $U = 0.25$. This is due to the fact that, as shown in the insets, for moderate values of the potential U , exactly two incident modes belonging to the zero-gap energy band are transmitted to the same band via two conducting channels. The same behavior of the transmission coefficient for small energies can be expected for all other metallic CNTs.

For large energies, $E \gtrsim 1.5$, we also observe a close similarity of $\mathcal{T}(E)$ for both values of the potential and all presented CNTs. This can be explained by the simple structure of the electron spectrum for large energy values: it is seen that the upper subbands of the energy bands have similar bell-like shapes. At the same time, for energy lying in the interval $0.5 \lesssim E \lesssim 1.5$, the energy dependences of \mathcal{T} are essentially different for different types of nanotubes. Moreover, as demonstrated in Fig. 4 for the CNTs of three considered types and close diameters $d \sim 12\text{\AA}$ (to recall, $d = a\sqrt{n^2 + m^2 + nm}/\pi$ for (n, m) CNTs [9]), the changes in behavior of $\mathcal{T}(E)$ can be organized in the following sequence: zCT \rightarrow (2m, m) CNT \rightarrow aCT. This is not at all surprising, taking into account that the corresponding sequence of the chiral angles is $0^\circ \rightarrow 19^\circ \rightarrow 30^\circ$. Thus, the differences in the behavior of electron conductance in the three types of CNT should be observed in measurements of source-to-drain current under varied gate voltage (playing the role of step potential) only in the energy range $1.3 \div 4$ eV. Our calculations show that the increase of the diameter of CNT leads to the smoothness of the dependences of $\mathcal{T}(E)$ and, therefore, reduces the differences between the process of electron transmission in different nanotubes. Thus, observable variations in $\mathcal{T}(E)$ and, therefore, electron conductance with nanotube types can be expected only for rather narrow nanotubes with diameters of up to 30\AA .

V. CONCLUSIONS

In conclusion, we note that we considered the transmission coefficients for achiral and chiral CNTs of any diameter with the help of matching the wave functions on the interface between the regions with zero and nonzero site energies. We used the exact solutions of the model Hamiltonian for the description of π electron states in ideal carbon achiral and chiral nanotubes. It is shown that the difference between the dependences of the transmission coefficients for different types of CNTs is well pronounced within the energy range $1.3 \div 4$ eV for narrow nanotubes with diameters of up to 30\AA and, most likely, can be observed in the course of the experimental investigations.

-
- [1] S. IJIMA, Helical microtubules of graphitic carbon, *J. Nature*, **354**, 56 (1991).
 - [2] D. A. GOMEZ-GUALDRÓN, J. C. BURGOS, J. YU, and P. B. BALBUENA, Carbon Nanotubes: Engineering Biomedical Applications, In: *Progress in Molecular Biology and Translational Science* (Editor: Antonio Villaverde,), Academic Press, **104**, 175-245 (2011).
 - [3] X. GAO, X. DU, T. S. MATHIS, M. ZHANG, X. WANG, J. SHUI, YU. GOGOTSI and M. XU, Maximizing ion accessibility in MXene-knotted carbon nanotube composite electrodes for high-rate electrochemical energy storage. *Nat Commun.*, **11**, 6160 (2020).
 - [4] M. ŚWINIARSKI, A. DUŻYŃSKA, A. P. GERTYCH, K. CZERNIAK-ŁOSIEWICZ, J. JUDEK, and M. ZDROJEK, Determination of the electronic transport in type separated carbon nanotubes thin films doped with gold nanocrystals, *Sci. Rep.*, **11**, 16690 (2021).
 - [5] B. LIU, F. WU, H. GUI, M. ZHENG, and C. ZHOU, *ACS Nano*, **11**, 31 (2017).
 - [6] V. SCHROEDER, S. SAVAGATRUP, M. HE, S. LIN, and T. M. SWAGER, *Chem. Rev.*, **119**, 599 (2019).
 - [7] G. HILLS, C. LAU, A. WRIGHT, S. FULLER, M. D. BISHOP, T. SRIMANI, P. KANHAIYA, R. HO, A. AMER, Y. STEIN, D. MURPHY, ARVIND, A. CHANDRAKASAN, and M. M. SHULAKER, *Nature*, **572**, 595 (2019).
 - [8] R. SAITO, M. FUJITA, G. DRESSELHAUSE, and M.S. DRESSELHAUSE, *Phys. Rev. B*, **46**, 1804 (1992).
 - [9] R. SAITO, G. DRESSELHAUSE, and M.S. DRESSELHAUSE, *Physical properties of Carbon Nanotubes*, Imperial College Press, UK 1998.
 - [10] T. ANDO, *J. Phys. Soc. Jpn.* **74**, 777 (2005).
 - [11] L. BREY and H. A. FERTIG, *Phys. Rev. B* **73** (2006) 235411.
 - [12] N. M. R. PERES, F. GOINEA, and A. H. CASTRO NETO, *Phys. Rev. B*, **73**, 125411 (2006).
 - [13] N. M. R. PERES, A. H. CASTRO NETO, and F. GOINEA, *Phys. Rev.*, **73**, 195411 (2006).
 - [14] L. MALYSHEVA and A. ONIPKO, *Phys. Rev. Lett.* **100**, 186806 (2008).
 - [15] A. ONIPKO, *Phys. Rev. B* **78**, 245412 (2008).
 - [16] K. WAKABAYASHI, K. SASAKI, T. NAKANISHI, and T. ENOKI, *Sci. Techn. Adv. Mat.* **11**, 054504 (2010).
 - [17] R. SAITO, A. R. T. NUGRAHA, E. H. HASDEO, N. T. HUNG, and W. IZUMIDA, *Top. Curr. Chem. (Z)*, **375**, 7 (2017).
 - [18] L. MALYSHEVA and A. ONIPKO, *Phys. Status Solidi B*, 1700248 (2017).
 - [19] V. A. SAROKA, M. V. SHUBA, and M. E. PORTNOI, *Phys. Rev. B*, **95**, 155438 (2017).
 - [20] N. R. SADYKOV, E. T. MURATOV, I. A. PILIPENKO, and A.V. APOROSKI, *Physica E*, **129**, 114071 (2020).
 - [21] F. YANG, X. WANG, D. ZHANG, J. YANG, D. LUO, Z. XU, J. WEI, J.-Q. WANG, Z. XU, F. PENG, X. LI, R. LI, Y. LI, M. LI, X. BAI, F. DING, and Y. LI, *Nature*, **510**, 522 (2014).
 - [22] SH. ZHANG, L. KANG, X. WANG, L. TONG, L. YANG, Z. WANG, K. QI, SH. DENG, Q. LI, X. BAI, F. DING, and J. ZHANG, *Nature*, **543**, 234 (2017).
 - [23] L. MALYSHEVA, Solution of the Spectral Problem for (2m,m) Carbon Nanotubes by Green's Function Method, *Physica Status Solidi B*, 2100264 (2021), <https://doi.org/10.1002/pssb.202100264>.
 - [24] YU. KLYMENKO, L. MALYSHEVA, and A. ONIPKO, *Physica Status Solidi B*, **245**, 2181 (2008).
 - [25] L. MALYSHEVA, E. PETRENKO, and A. ONIPKO, Interband transmission in armchair graphene ribbons with a step-like profile of potential energy: Relevance to Klein's tunneling, *Physica Status Solidi B*, **246**, 2405 (2009).
 - [26] YU. KLYMENKO and O. SHEVTSOV, *Eur. Phys. J. B* **69**, 383; **72**, 203 (2009).
 - [27] YU. O. KLYMENKO, *Low Temp. Phys.* **37**, 496 (2011).
 - [28] L. MALYSHEVA and A. ONIPKO, Electron transmission through step-like potential in armchair and zigzag graphene nanoribbons: Comparison of different interfaces, *Physica Status Solidi B*, **252**, 1981 (2015).
 - [29] B. L. SHARMA, *Eur. Phys. J. B* **91**, 84 (2018).
 - [30] L. MALYSHEVA and A. ONIPKO, *Physica Status Solidi B* **255**, 1700248 (2018).
 - [31] L. CHICO, L. X. BENEDICT, S. G. LOUIE, and M. L. COHEN, Quantum conductance of carbon nanotubes with defects, *Phys. Rev. B*, **54**, 2600 (1996).